Electrical Stimulation Based Statistical Calibration Model

For MEMS Accelerometer And Other Sensors

by

Ishaan Bassi

A Thesis Presented in Partial Fulfillment
of the Requirements for the Degree
Master of Science

Approved July 2020 by the
Graduate Supervisory Committee:

Sule Ozev, Chair
Jennifer Blain Christen
Dragica Vasileska

ARIZONA STATE UNIVERSITY

August 2020

ABSTRACT

Micro Electro Mechanical Systems (MEMS) based accelerometers are one of the most commonly used sensors out there. They are used in devices such as, airbags, smartphones, airplanes, and many more. Although they are very accurate, they degrade with time or get offset due to some damage. To fix this, they must be calibrated again using physical calibration technique, which is an expensive process to conduct. However, these sensors can also be calibrated infield by applying an on-chip electrical stimulus to the sensor. Electrical stimulus-based calibration could bring the cost of testing and calibration significantly down as compared to factory testing. In this thesis, simulations are presented to formulate a statistical prediction model based on an electrical stimulus. Results from two different approaches of electrical calibration have been discussed. A prediction model with a root mean square error of 1% has been presented in this work. Experiments were conducted on commercially available accelerometers to test the techniques used for simulations.

ACKNOWLEDGMENTS

Firstly, I would like to thank my advisor Dr. Sule Ozev for supporting me on this research project and guiding me through my master's degree. I would also like to thank my other committee members Dr. Jennifer Blain Christen and Dr. Dragica Vasileska, who allowed me to work with them. I would also like to thank the team at Alphacore for helping during the project.

I would like to thank my parents Mrs. Arun Bala and Mr. Ravinder Bassi, and also my other family members for encouraging and always backing me to continue my studies. I would like to thank Mr. Manpreet Malhotra for guiding and pushing me to do research and helped me to get to ASU.

Finally, I would like to thank all my friends back in India and here at ASU for always being there when needed.

TABLE OF CONTENTS

Page

LIST OF TABLES iv

LIST OF FIGURES v

CHAPTER

1 INTRODUCTION 1

1.1 Background 1

1.2 Mems Accelerometer 4

1.3 Capacitive MEMS Accelerometer 7

1.4 Research Goals 10

1.5 Previous Work 10

1.6 Scope Of The Thesis 15

1.7 Summary Of The Chapter 16

2 MATLAB/SIMULINK SIMULATION MODEL DESIGN 17

2.1 Simulink Accelerometer Model 17

2.2 Parameter Extraction 22

2.3 Summary Of The Chapter 24

3 CALIBRATION MODEL FORMULATION BASED ON SIMULATIONS 25

3.1 Electrically Inducing DC Offset 25

3.2 Sensitivity Degradation Model 29

3.3 Summary Of The Chapter 32

CHAPTER Page

4 ACCELEROMETER HARDWARE TESTING 33

4.1 Only DC Offset Experiment 33

4.2 AC And DC Electrical Stimulus 34

4.3 Fixed AC And Different DC Offsets 35

4.4 Summary Of The Chapter 38

5 CONCLUSION AND FUTURE WORK 39

REFERENCES 41

LIST OF TABLES

Table Page

2.1 Design Parameters 21

4.1 DC Offset Sensitivity Comparison 34

4.2 AC And DC Stimulus For Different Operating Voltages 35

LIST OF FIGURES

Figure Page

1.1 Advantages And Disadvantages Of Different Types Of Accelerometers [3]..............4

1.2 Lumped Element System 5

1.3 Types Of Capacitive Transducer Structures 7

1.4 Capacitive MEMS Structure 8

1.5 Accelerometer Under Applied External Force...9

1.6 Accelerometer Excited By Electrostatic Force 11

1.7 Multi Partition Design For Bist [4] 13

1.8 Fabrication Mismatch [7]..14

1.9 Prediction Model Using Pull-In Technique [7]...14

2.1 Physical Acceleration Stimulus...17

2.2 Simulink Model For Physical Excitation Of Accelerometer 18

2.3 Electrical Stimulus Of Accelerometer..19

2.4 Simulink Model For Electrical Stimulus 19

2.5 Input Voltage Signal (50hz)..20

2.6 Output Delta Capacitance (100hz) 20

2.7 Output Response Of The Model...22

3.1 Sensitivity Vs Samples (Without And With An Offset Of 50nm) 26

3.2 Algorithm For Parameter Extraction Of Incremental Values Of DC Offsets.............27

3.3 Sensitivity Vs Electrical Response 28

Figure Page

3.4 Delta Change Parameter Extraction Algorithm 30

3.5 Delta Change In Electrical Parameters(Ω, C & Φ) Vs Delta Change In Sensitivity 31

4.1 Test Setup.. 33

4.2 Frequency Response For Different DC Offsets 36

4.3 (A) 0voff, (B) 1voff & (C)1.5voff.. 36

4.4 AC Response And DC Offset Vs Sensitivity (Sensor 1) 37

Chapter 1 INTRODUCTION

1.1 Background

With advances made in miniaturizing electronics, sizes of physical sensors have also reduced significantly, all thanks to MEMS (Micro Electro Mechanical Systems). The MEMS comprises electronic and mechanical (moving) components, which perform different functions such as, transduction, actuation, signal processing. Reduction in size and new designs for various applications has increased the use of MEMS-based sensors in many devices such as, Smartphones, Automobile, personal health care devices.

MEMS are fabricated using the same techniques used for CMOS electronic devices, such as etching, lithography patterning, material deposition [1]. Lithography is a technique used to make patterns of a required design for the sensor onto the semiconductor wafer, which then can be used as a reference to etch out some material or to deposit a patterned thin film. A combination of these steps is used to make a three-dimensional structure of the MEMS device. One of the best examples is the formation of free suspended beams used in a MEMS accelerometer, which is the focus of this thesis work. Most of the mechanical structures in MEMS are made out of semiconductor material such as, silicon, polysilicon, silicon oxide. This because of the ease of fabrication due to the well-established fabrication technology for silicon. However, other materials may also be used depending on the application and MEMS structure. PZT is used for its piezoelectric property, which is used in MEMS microphones. The benefit of using the CMOS fabrication technique is that the sensors can be fabricated along with other electronic components such as, modulators, amplifiers that are used in the operation of the overall electronic system.

The most critical performance metric of a MEMS sensor is its sensitivity. The sensitivity of a sensor is defined as the change in the output electrical variable with respect to change in the physical stimulus the sensor is designed to measure. For instance, in the case of the capacitive MEMS accelerometer, the sensitivity is defined as the change in the differential capacitance with respect to change is acceleration. The differential capacitance is also measured using electronic circuits via capacitance-to-voltage conversion. Thus, the sensitivity of the overall sensor system, including the electronic subsystem, can also be defined as the change in the output voltage with respect to change in acceleration.

Since sensors have mechanical structures as their core functioning elements, they are prone to structural deformities or natural variations of control variables induced during production. Thus, the initial sensitivity of each manufactured device will deviate from its design target. These deviations are deemed as process variations and need to be measured and calibrated post-production using special automated test equipment (ATE). The ATE for MEMS accelerometers includes functional units that are capable of moving the sensor device in all three dimensions with a pre-determined acceleration amount. The output voltage is measured by the electronic measurement unit of the ATE to calculate the sensitivity. The calculated sensitivity is passed on the digital subsystem of the MEMS accelerometer to calibrate the voltage readings back into the acceleration domain. Process variations may account for as much as 30% variation in the sensitivity of the accelerometer [15]. The standard for calibration, which is referred to as the NIST traceability standard [18], is to measure this sensitivity to within 1% error.

In addition to the process variations, which are formed during manufacturing, the material properties of sensor devices degrade or shift over time due to wear out mechanisms [16]. Thus, even if a sensor device is accurately calibrated post-production, this accuracy may degrade over time as the device is subjected to harsh conditions, including high humidity, high temperature, and high levels of acceleration [17]. These changes in mechanical properties cause deviation from the initial sensitivity provided by the manufacturer.

The goal of this thesis work is to develop a mechanism for measuring and calibrating sensor sensitivity degradation in the field without using bulky and expensive equipment and without having to remove the sensor device from the field. A statistical model is formulated to correlate the changes in the MEMS accelerometer sensitivity to its response to a pre-defined set of electrical stimuli. The electrical stimuli that best correlates to physical behavior for this purpose have been developed in [15]. This population-based model achieves sensitivity calibration with no physical stimulus within 3% over a wide range of process variations. In this thesis, our goal is to apply the same or similar electrical stimuli and correlate the change in sensitivity to change in electrical response to enable a more accurate calibration in the field after the sensitivity is measured via mechanical stimuli post-production. This in-field calibration approach will enable the NIST traceability of MEMS accelerometers for safety critical applications [18].

1.2 MEMS accelerometer

Accelerometers are very widely used sensors in several areas, such as in cars to deploy airbags in smartphones to detect the orientation of the phone, aviation, biosensors. An accelerometer is a device that provides the data about the motion of a device that they are installed inside. There are various types of accelerometers such as, piezoelectric, piezoresistive, capacitive, thermal, tunneling, and optical, which are used for transducing this motion of a proof mass (Figure 1.1) [2]. Accelerometers are also designed to measure the acceleration in multiple directions; for example, there are single axis, dual-axis, and triple axis accelerometers. The focus of this work will be on capacitive accelerometers as they are the most widely used and commercially available sensors, because of the ease interpretation. Also, they are relatively cheaper than others.

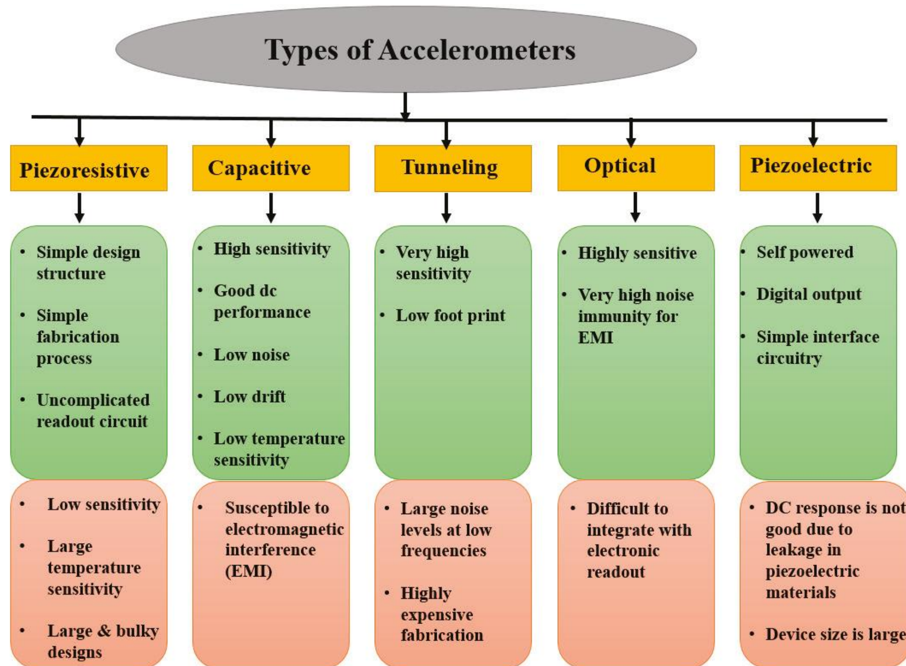

Figure 1.1 Advantages and disadvantages of different types of accelerometers [3]

The basic structure of a capacitive MEMS accelerometer consists of a proof mass suspended by a spring and connected to a metal plate that is situated within two fixed plates. This proof mass displaces when there is an external force applied to the device in which it is installed. The motion of the proof mass also moves the metal plate, moving it closer to one of the fixed plates and away from the other fixed plate depending on the direction of the acceleration. From an electrical perspective, the fixed plates and the movable plate form two capacitances. The motion of the proof mass then increases one capacitance and reduces the other, basically changing the differential capacitance. This differential capacitance is measured by employing a capacitance-to-voltage converter circuit, which converts this physical parameter to an electrical signal. The electrical signal is further processed and translated into the digital domain, which then is converted into a readable acceleration value.

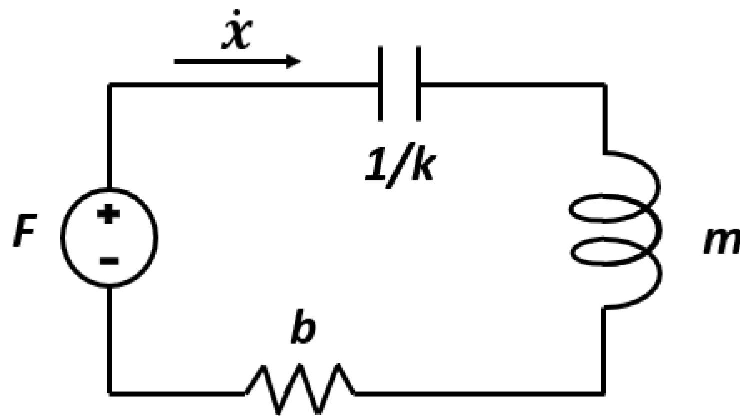

Figure 1.2 Lumped element system

The essential operation of an accelerometer can be defined in the form of a second-order lumped-element system. Figure 1.2 shows the spring damper system, which is used

to derive the second-order equation that defines the relation between the displacement of the proof mass and the acceleration that is applied to it. The parameters in the model correspond to the physical parameters of the accelerometer. ***F*** is the external force applied to the accelerometer, ***k*** is the spring constant, ***m*** is the mass of the proof mass, and ***b*** is the damping coefficient of the air where the mass oscillates [1]. $\dot{x}$ corresponds to the velocity of the proof mass due to the external force. The second-order equation (Eq 1.7) can be derived from the lumped system [3],

$$F_{applied} = ma_{applied} \quad \text{Eq. 1.1}$$

$$F_{spring} = kx \quad \text{Eq. 1.2}$$

$$F_{damping} = b\dot{x} \quad \text{Eq. 1.3}$$

By balancing all the forces in the system, the relation between the displacement and the external acceleration can be formulated (Eq 1.5).

$$F_{applied} - F_{spring} - F_{damping} = m\ddot{x} \quad \text{Eq. 1.4}$$

$$m\ddot{x} + b\dot{x} + kx = ma_{applied} \quad \text{Eq. 1.5}$$

The transfer function of the system in the frequency domain can be derived as in Eq. 1.6 and Eq. 1.7,

$$ms^2x(s) + bsx(s) + kx(s) = ma(s) \quad \text{Eq. 1.6}$$

$$\frac{x(s)}{a(s)} = \frac{1}{s^2 + \frac{b}{m}s + \frac{k}{m}} = \frac{1}{s^2 + \frac{\omega_0}{Q}s + \omega_0^2} \quad \text{Eq. 1.7}$$

The resonant frequency of the accelerometer can be calculated from the transfer function expression, the resonant frequency, ω_0, is represented in the form of k and m, as shown in Eq 1.8.

$$\omega_0 = \sqrt{k/m} \qquad \text{Eq. 1.8}$$

For frequencies below ω_0 the relation between acceleration and displacement can be expressed as in Eq. 1.9,

$$x = \frac{ma}{k} \qquad \text{Eq. 1.9}$$

1.3 Capacitive MEMS accelerometer

Among the various methods of measuring the displacement of the proof mass in an accelerometer, differential capacitance measurement is the most prevalent technique [1]. While there are multiple types of physical structures used, such as, parallel plate capacitor, interdigitated fingers, as shown in Figure 1.3, similar methods are used for the measurement of the differential capacitance [4]

Figure 1.3 Types of capacitive transducer structures

Figure 1.4 shows the basic structure of a capacitive accelerometer. A suspended beam is placed between the two fixed conductive plates (P_1, P_2). The proof mass (M) is connected to this suspended beam. This proof mass moves up or down depending on the amplitude and direction of the externally applied force. Initially, the gap between the top plate and the proof mass and the gap between the bottom plate and the proof mass is the same (d_0). This forms a capacitive structure with two capacitances, top, and bottom. The area (A) of the top and the bottom plates is the same. The gap between the three plates is filled with air whose dielectric constant is represented by (ϵ_0).

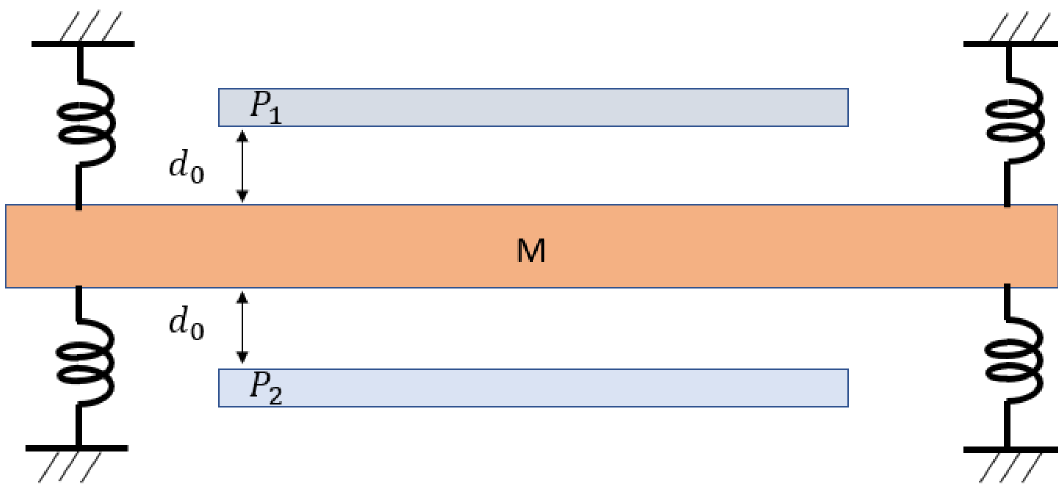

Figure 1.4 Capacitive MEMS structure

When there is a displacement of the mass plate caused due to an external force, there is an offset in the gaps between the plates resulting in a difference between the two capacitances. This differential capacitance can be measured using a mixed-signal electronic circuit. The capacitance for a parallel plate capacitor is given by Eq. 1.10,

$$C = \frac{\epsilon_0 A}{d_0} \qquad \text{Eq. 1.10}$$

The variable in Eq. 1.10 that will be affected by the displacement of the mass is d_0. If the mass moves a distance x in one direction, the net offset in the gap becomes $2x$. The change in capacitance can be calculated using Eq 1.11,

$$C_1 - C_2 = \frac{\epsilon_0 A}{d_0+x} - \frac{\epsilon_0 A}{d_0-x} = \frac{2\epsilon_0 Ax}{d_0^2-x^2} \qquad \text{Eq. 1.11}$$

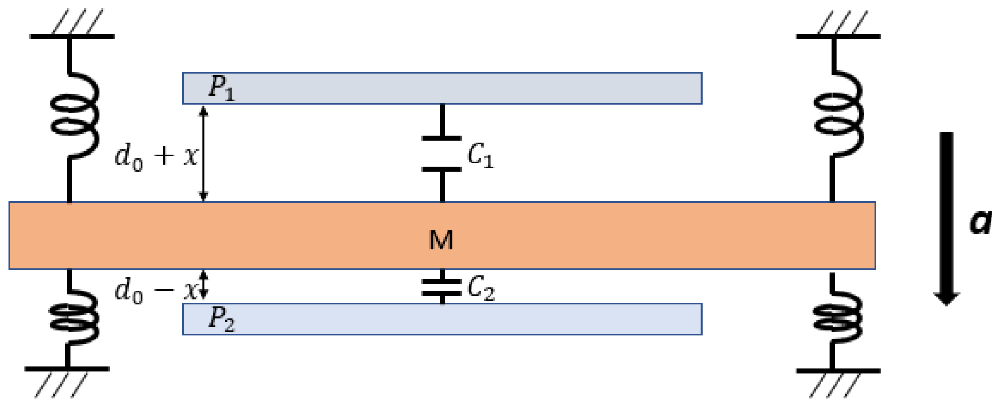

Figure 1.5 Accelerometer under applied external force

The displacement x is generally relatively very small (less than 10%) compared to the gaps, d_0. Thus, the expression for the differential capacitance can be simplified to Eq 1.12,

$$\Delta C = \frac{\epsilon_0 Ax}{d_0^2} \qquad \text{Eq. 1.12}$$

$$x = \frac{d_0^2 \Delta C}{\epsilon_0 A} \qquad \text{Eq. 1.13}$$

Using Eq 1.9 and Eq 1.13 an expression for the relationship between differential capacitance and acceleration can be derived in Eq 1.14,

$$a = \frac{k}{m} . \frac{d_0^2}{\epsilon_0 A} \Delta C \qquad \text{Eq. 1.14}$$

1.4 Research goals

As the sensor ages [12,13], its physical parameters start to deviate from its initial value, which results in a shift in its sensitivity. Several techniques have been proposed for in-field calibration of MEMS accelerometers by applying an electrical stimulus to the sensor [8].

The goal of this research work is to develop a prediction model that can predict the sensitivity of an accelerometer in-field, without it being taken back to a testing facility. This research work focuses on the following areas:

- Developing a set of simulation and statistical prediction models for a population of sensors.
- Implementing the proposed approach on commercially available sensors for hardware.

1.5 Previous work

There are multiple methods for testing and calibrating a MEMS accelerometer, one of which is physical testing done during the production of the sensors. This type of testing uses external physical stimulus to excite the accelerometer and get a correlation between the applied acceleration and output voltage. Physical calibration systems are used to define the sensitivity of an accelerometer. However, there are many other nonphysical stimulus-based methods in which there is no need to apply an external force—just the analysis of the electrical response of the sensor caused by an electrical stimulus to the accelerometer.

In [6], access to internal structures is enabled through self-test pins to enable electrical excitation of the MEMS accelerometer after packaging. These self-test pins are the most commonly available in commercial sensors to sensor verify simple performance parameters, such as pull-in voltage for the manufactured sensors or to check for catastrophic structural failures, such as an obstruction that prevents the movement of the proof mass [9] or a structural defect in the spring.

When an electrical signal is applied across the parallel plates of a MEMS accelerometer, an electrostatic force is generated between the plates. This electrical force is used to emulate an external physical force due to the acceleration of the proof mass. The electrical force due to an applied voltage(V) [5] can be calculated with Eq. 1.15,

$$F_{electrical} = \left(\frac{1}{2}\right).C.\frac{V^2}{d} = \frac{\epsilon_0 A}{2}\left(\frac{V}{d}\right)^2 \qquad \text{Eq. 1.15}$$

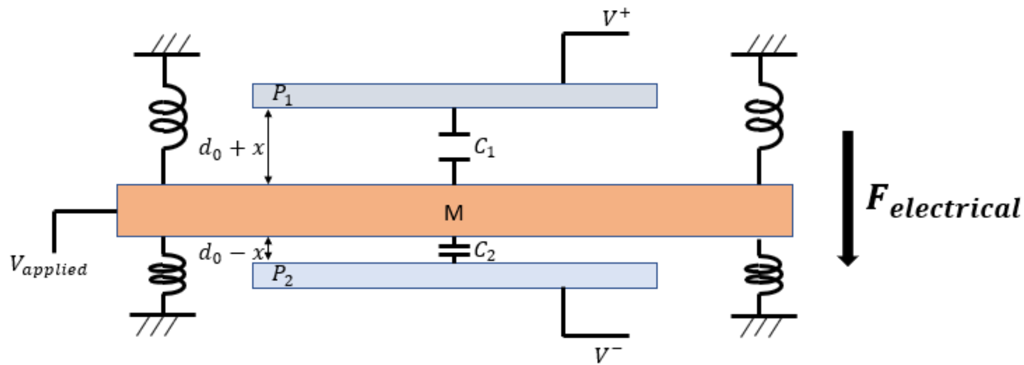

Figure 1.6 Accelerometer excited by electrostatic force

The ability to emulate a physical force using electrical means enables the development of built-in self-test technique (BIST) techniques that rely only on electronic components. Various researchers have focused on the development, evaluation, and implementation of BIST mechanisms for MEMS accelerometers.

In [5], an electrical stimulus based technique was developed to electrically characterize and diagnose the mechanical parameters of the cantilever beam of a MEMS accelerometer. These parameters include mass, spring constant, and damping coefficient. To achieve this goal of mechanical parameter prediction, a gradient sweep algorithm was developed in which frequency sweep was done in a specific range to find the resonant frequency of the sensor. 70 sensor models were generated using the Monte Carlo simulation. By doing gradient frequency sweep, the error in predicted and actual value was calculated. Using the results from this training set, a nonlinear model based on the MARS model was developed. Furthermore, RMS error values were calculated from a test set of 30 devices. An estimation error 5% was reported for the mechanical parameters.

To detect global and local defects in the structure of a MEMS accelerometer, a new mechanical design modification was proposed in [4]. Partitioning of the fixed plates was proposed so that separate electrical signals can be applied at different regions, and deformities can be predicted. In this design, the fixed plates were split into 2 or 3 sections, as shown in figure 1.7, to apply different polarities of voltages across the capacitors, which resulted in 4 differential capacitances instead of 2 used in standard designs. By doing so, when the output voltages are compared for the offsets between the capacitance pairs C1-C3 and C2-C4, any local defects can be detected. Any faults will be reflected in the results if there is an offset in the symmetry. The 3-section design was used to identify any global defects that may have occurred across the sensor.

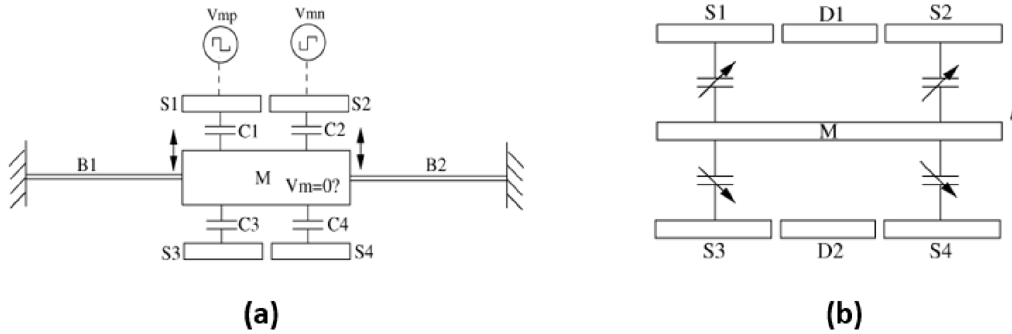

Figure 1.7 Multi partition design for BIST [4]

When a voltage that is applied across the parallel plates of a capacitor reaches a critical value, a pull-in voltage is the maximum amount of voltage that can be applied across the capacitor plates without getting a maximum deflection equal to the gap. Pull-in voltage is defined by Eq 1.16.

$$V_{Pull-in} = \sqrt{\frac{\frac{8}{27}d_0^3 k}{\epsilon_0 w l}} \qquad \text{Eq. 1.6}$$

An electrical calibration technique for a MEMS accelerometer was proposed in [7], which was based on mechanical structure parameter estimation using the pull-in voltage data of the MEMS accelerometer mechanical structure. Due to the errors caused during the fabrication of the fixed plates and the movable mass, a mismatch could occur in the gaps between the two plates and the mass, as seen in figure 1.8.

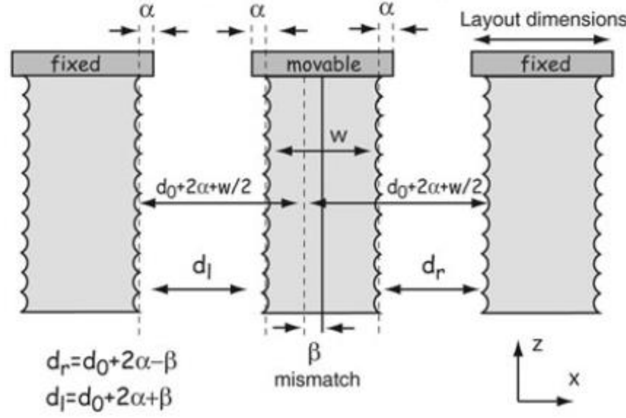

Figure 1.8 Fabrication mismatch [7]

A model was created based on the measured pull-in voltages of the left and the right section. An iterative method was used to find the parameter α and β by matching the values of calculated and measured pull-in voltage and resonant frequency. Figure 1.9 shows the equations of the proposed model.

Model		Step 1 $\alpha = 0$ $\beta = 0$ $E = 170$ GPa	Step 2 $\alpha = 209$ nm $\beta = 0$ $E = 170$ GPa	Step 3 $\alpha = 209$ nm $\beta = 25$ nm $E = 162$ GPa	Step 4 $\alpha = 184$ nm $\beta = 25$ nm $E = 160$ GPa
Mechanical domain	$k(\alpha, E) = -\frac{E}{8.8\times10^4}\alpha + \frac{E}{170\times10^9}$ (N/m)	1 N/m	0.596 N/m	0.568 N/m	0.60 N/m
	$m(\alpha) = -0.75 \times 10^{-3}\,\alpha + 1 \times 10^{-9}$ (Kg)	1 µg	0.84 µg	0.84 µg	0.86 µg
	$f_r(\alpha, E) = \frac{1}{2\pi}\sqrt{\frac{k(\alpha,E)}{m(\alpha)}}$ (Hz)	**5,107 Hz**	**4,205 Hz**	**4,116 Hz**	**4,198 Hz**
Electrical domain	$d_r = 2 \times 10^{-6} + 2\alpha - \beta$ (m)	2 µm	2.418 µm	2.393 µm	2|343 µm
	$d_l = 2 \times 10^{-6} + 2\alpha + \beta$ (m)	2 µm	2.418 µm	2.443 µm	2.393 µm
	$N = 12$ (number of parallel capacitors)	12	12	12	12
	$l = (282 \times 10^{-6} - 2\alpha)\,N$ (m)	3.384 mm	3.379 mm	3.379 mm	3.379 mm
	$w = 10.6 \times 10^{-6}$ (m)	10.6 µm	10.6 µm	10.6 µm	10.6 µm
Pull-in	V_{cr} (α, β, E) (Eq. 1)	**2.770 V**	**2.796 V**	**2.687 V**	**2.682 V**
	V_{cl} (α, β, E) (Eq. 1)	**2.770 V**	**2.796 V**	**2.772 V**	**2.768 V**
Measurements	Right pull-in	$V_{pr} = 2.683$ V			
	Left pull-in	$V_{pl} = 2.770$ V			
	Resonance frequency	$f_0 = 4{,}205$ Hz			

Figure 1.9 Prediction model using pull-in technique [7]

A fully electrical test based sensitivity prediction method was proposed in [9,10], the goal of the method was to train the model electrical response of the system, and analytical sensitivity expressions. A finite element analysis simulation was done for a set

of models generated with the help of Monte Carlo simulation. The sensitivity model was created based on four different sensitivities calculated using mechanical parameters. The prediction model was then trained using sensor population, which had variation in mechanical parameters over a specified spread. The variations were considered both for global data as well as for inter die sensor sets. Here also, the prediction model is dependent on the knowledge of the physical parameters of the sensors. This complicates the model because of the number of variables present in the model.

A BIST circuitry was proposed in [11] to implement electrical response only calibration of the MEMS accelerometer. The proposed prediction model had no dependency on the knowledge of physical parameters to train. A linear model was generated based on the electrical output response of the sensor such as, phase shift, high and low-frequency response, and DC offset. This makes the prediction way less complicated when compared to other previous works.

1.6 Scope of the thesis

This thesis will focus on developing statistical models that correlate the electrical response of a MEMS sensor to the change in its physical sensitivity. This thesis will cover these topics:

1. A simulation model for the MEMS accelerometer is generated using the MATLAB/Simulink software. This model determines the output response of the MEMS device based on both physical and electrical stimulation.
2. Simulating the models for different electrical test methods and creating a statistical model of prediction.

3. Hardware testing of commercially available accelerometers.

1.7 Summary of the chapter

1. Background of MEMS devices and the need for in-field calibration.
2. Theoretical working of MEMS accelerometers.
3. Structure and equation governing capacitive transduction in MEMS accelerometers.
4. Previous research on electrical stimulation based calibration of accelerometers.
5. Scope of the thesis.

Chapter 2 MATLAB/SIMULINK SIMULATION MODEL DESIGN

2.1 Simulink accelerometer model

A MATLAB/Simulink model of an accelerometer was developed based on the second-order lumped model, that has been presented in the previous chapter. The Eq. 2.1 defines the transfer function of the system that was implemented. The model is dependent on the physical parameters, namely, spring constant (k), mass (m), damping coefficient (b), area of the plates (A) and gap (d_0) between the plates.

$$\frac{d^2x}{dt^2} = a - \frac{b}{m}\frac{dx}{dt} - \frac{k}{m}x \qquad \text{Eq. 2.1}$$

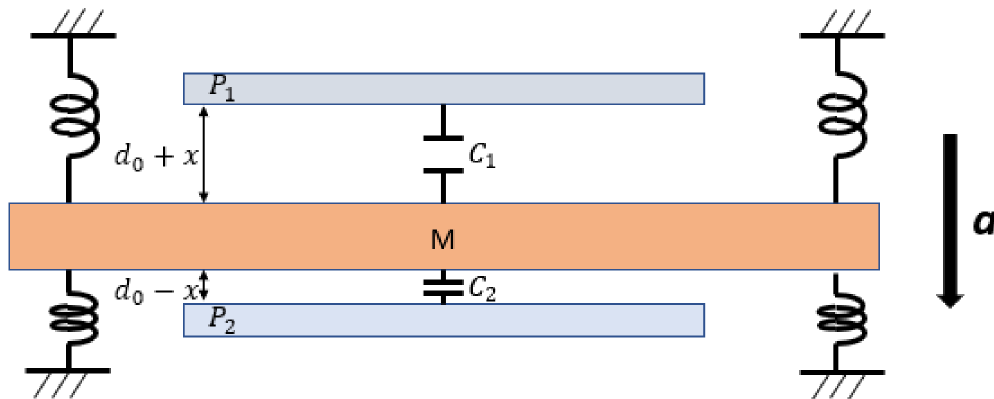

Figure 2.1 Physical acceleration stimulus

The physical-stimulus Simulink model was constructed to simulate the results of a physically excited proof mass, as shown in figure 2.1. This is a second-order closed-loop system. A sinusoidal acceleration pattern is applied as the physical input to the system. The output is the differential capacitance that is generated by the displacement of the proof mass [15]. The differential capacitance is calculation using Eq. 2.2,

$$\Delta C = \epsilon_0 A\left(\frac{1}{d_0 - x - \Delta} - \frac{1}{d_0 + x + \Delta}\right) \qquad \text{Eq. 2.2}$$

Where x is the displacement caused due to the acceleration and Δ is the delta at-rest gap differential between the plates that stems from process variations, potential structural deformities, and wear out.

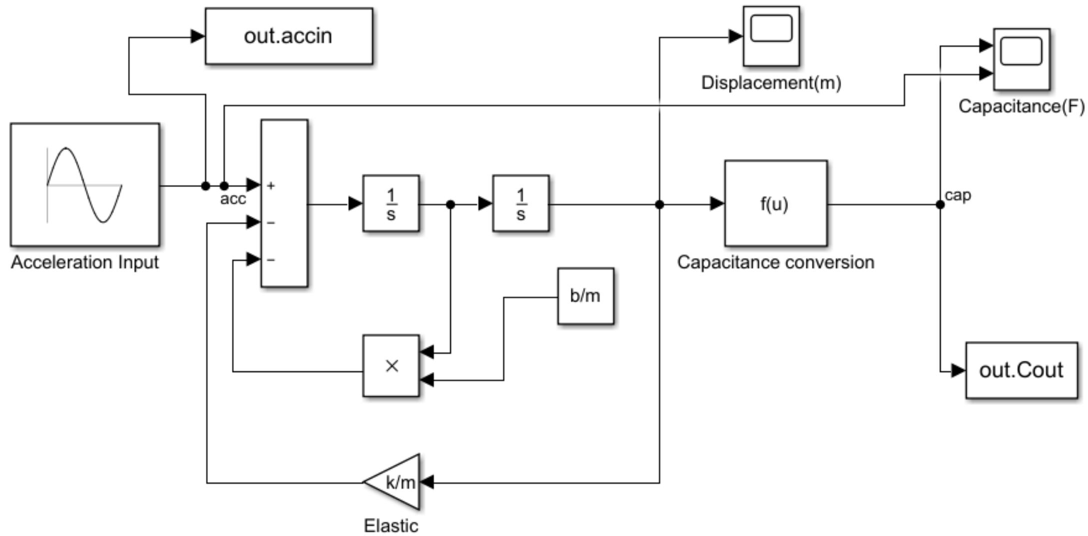

Figure 2.2 Simulink model for physical excitation of accelerometer

As discussed in Section 1.5, a force exerted due to an applied voltage can emulate into an acceleration of the proof mass as expressed in Eq 2.3. Thus, the second Simulink model was developed to simulate for this effect. The model simulates an electrical signal applied between the proof mass and one of the fixed plates, which causes a deflection of the proof mass. This deflection can then be translated into the change in capacitance at the output of the system. Eq. 2.3 represents the electrostatic force between one of the fixed plates and the movable plate due to an applied voltage, V . For the movable plate to settle, this force needs to be countered by the force generated due to the spring. Thus, any

displacement due to the electrostatic force will be strongly correlated to the physical parameters of the MEMS device.

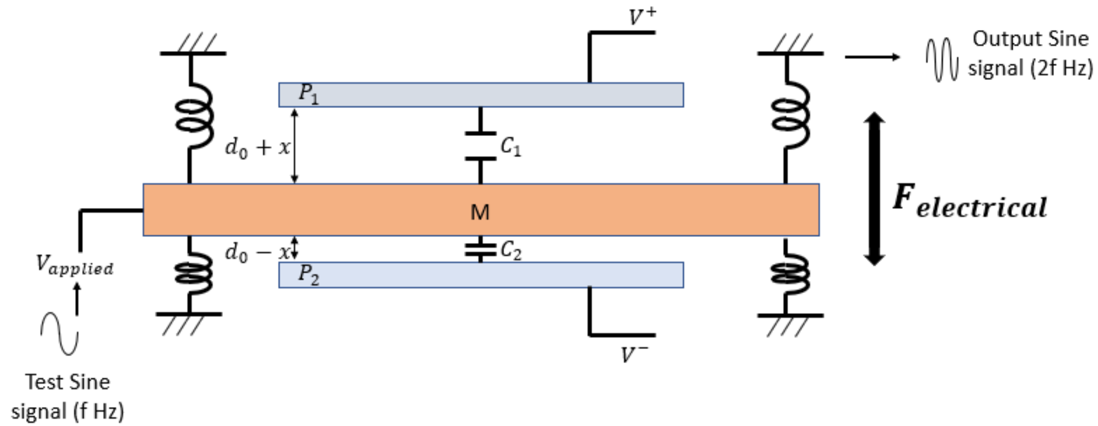

Figure 2.3 Electrical stimulus of accelerometer

$$F_{electrical} = \left(\frac{1}{2}\right).C.\frac{V^2}{d} = \frac{\epsilon_0 A}{2}\left(\frac{V}{d}\right)^2 \qquad \text{Eq. 2.3}$$

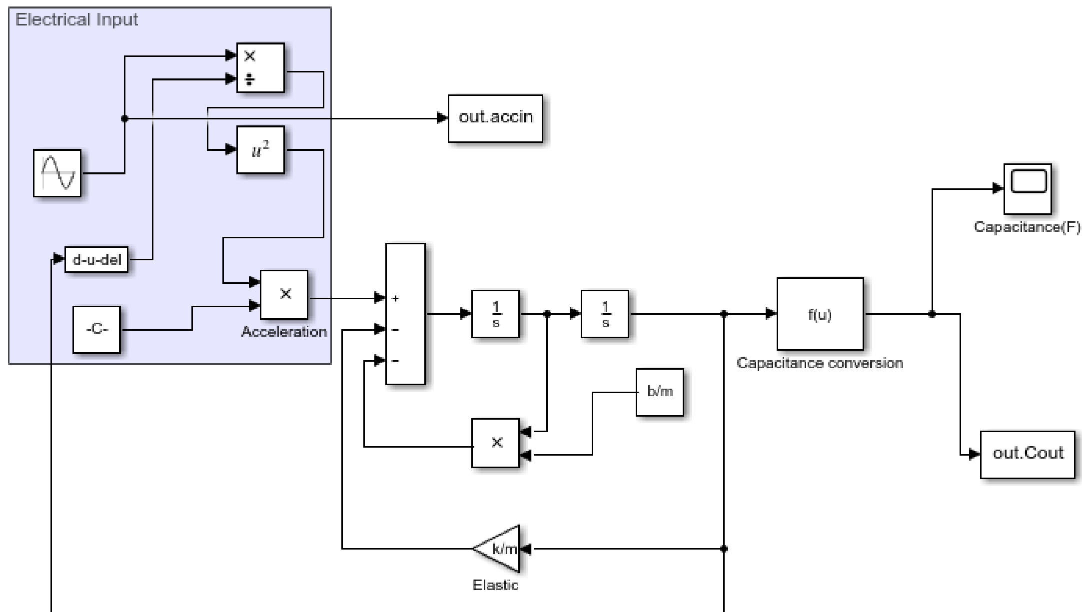

Figure 2.4 Simulink model for Electrical stimulus

If the electrical signal is a sinusoidal with a frequency of ω_0, Eq. 2.3 can be simplified as in Eq. 2.4 to observe the frequency effect of the applied signal. It should be noted from Eq. 2.4 that the acceleration signal equivalent to the applied voltage will be at twice the frequency of the input voltage electrical signal. This effect is illustrated in Fig. 2.5 and Fig. 2.6 that show the input electrical signal and the output differential capacitance.

$$F_{electrical} = \frac{\epsilon_0 A V^2}{2}[1 - \cos(2\omega t)] \qquad \text{Eq. 2.4}$$

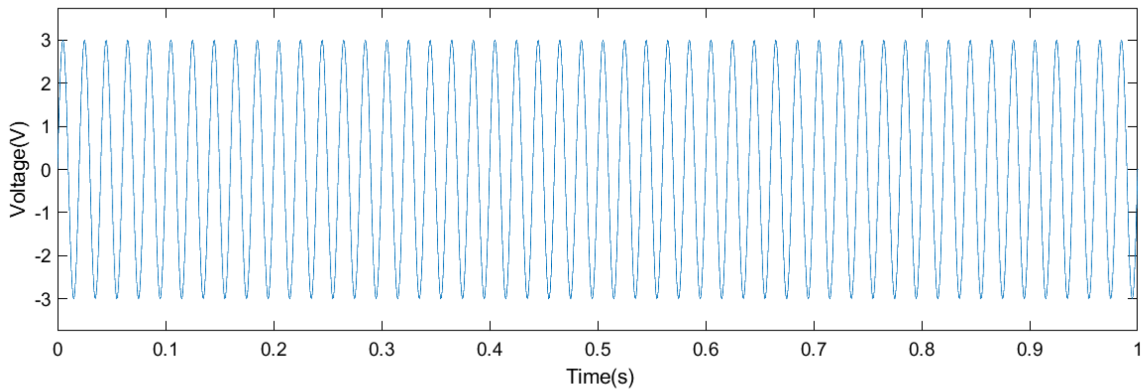

Figure 2.5 Input voltage signal (50Hz)

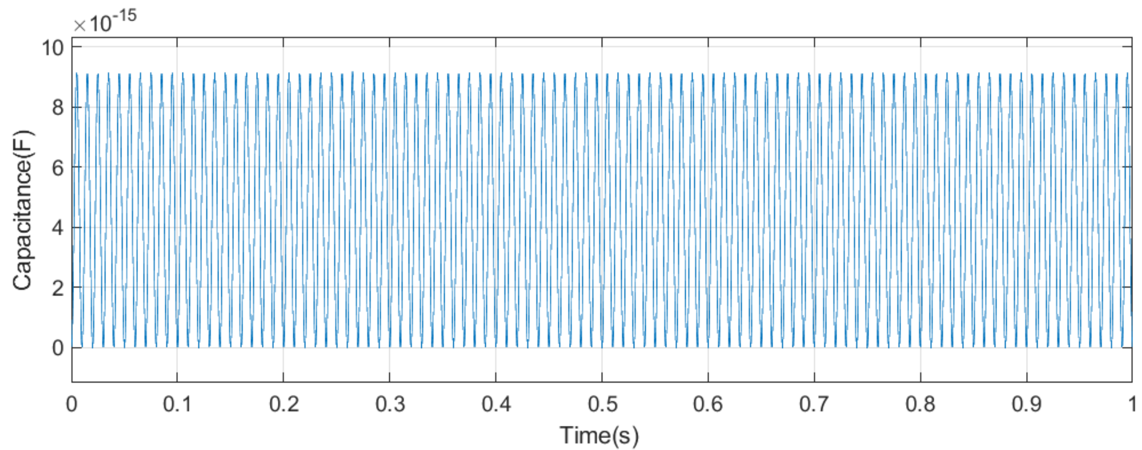

Figure 2.6 Output delta capacitance (100Hz)

In addition to doubling of the frequency, the differential capacitance also presents with a DC offset that is different than the resting offset due to process variations and aging. Thus, one cannot directly measure the internal offset by applying the electrical signal; it has to be inferred from multiple measurements. Eq. 2.4 also shows the first order (DC) and second-order (AC) terms [14] corresponding to these two effects.

The design parameters used for modeling the Simulink model are shown in Table 2.1.

Table 2.1 Design Parameters

Parameters	**Value**	**Units**
Mass (m)	3.3	Kg
Area (A)	60×10^{-9}	m^2
Spring Constant (k)	3.5	N/m
Gap (d)	1.7×10^{-6}	m
Damping Coefficient (b)	150.45×10^{-6}	$N\ s/m$
Permittivity (ϵ_0)	8.85×10^{-12}	F/m
Gravitational acceleration (g)	9.8	m/s^2

The transfer function and phase plots of the Simulink model for gap offsets $\Delta = 0\&50nm$ are shown in figure 2.7. It can be observed from this figure that the response of the system is different if the gap offset is shifted. A similar observation can be done if the input electrical signal has an additional DC component. Thus, we can conclude that the sensitivity of the MEMS accelerometer device depends not only on the manufacturing parameters of the device, but also on the external conditions, such as the applied DC offset and magnitude of the electrostatic force. This observation is the basis of the approach for formulating a model in this research. This offset could either be electrically induced or could be caused by the aging of the sensor or any accidental damage.

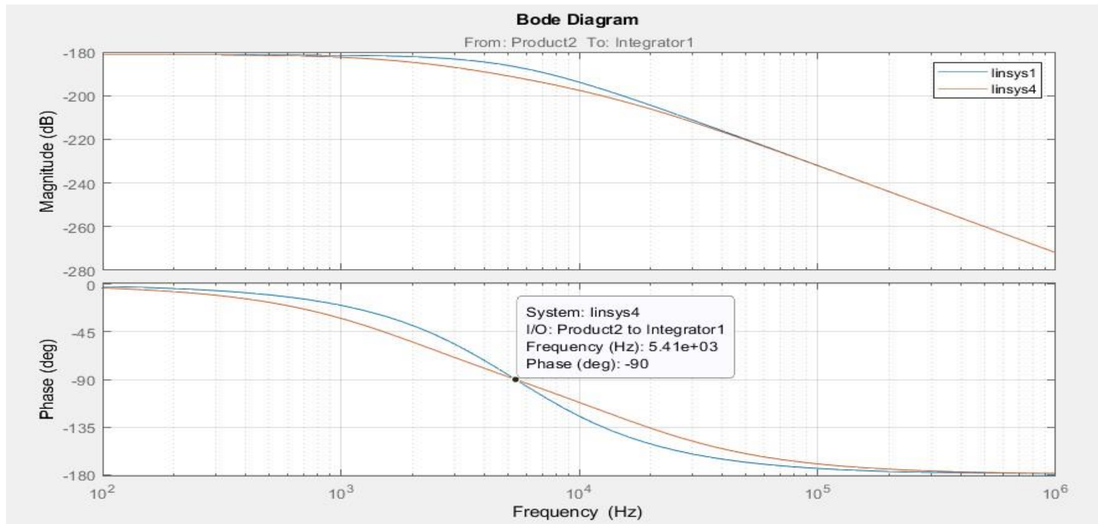

Figure 2.7 Output Response of the model

2.2 Parameter extraction

From these Simulink models, a few electrical parameters can be extracted that can be further used for constructing a statistical prediction model. The electrical parameters are defined in this section.

1. Frequency response

Due to the second order damping nature of the mass-spring apparatus, the response of the MEMS device will have frequency dependent characteristics. The magnitude of the response diminishes with increasing frequency of the applied signal. This effect is illustrated in Fig. 2.7. Fig. 2.7 shows the frequency response of two accelerometer simulation instances generated with two sets of process parameters. It can be observed from this figure that the frequency response of the two device instances differ. Thus, the MEMS device acts as a low-pass filter, whose electrical characteristics can be measured to construct a statistical model.

One of the variables that is used for statistical modeling will be the low frequency gain of this low-pass filter.

2. Cut-off frequency

Cut-off frequency is defined as the frequency at which the gain drops by 3dB. Intuitively, an electrical signal is applied to move the proof mass in the opposite direction to generate an equilibrium. If this electrical signal is an alternating signal, the movement will also be an alternating movement, albeit in the opposite direction. However, there is limit to how fast the proof mass can move. Hence, if the electrical signal is changed too rapidly, the proof-mass/spring system may not be able to response. In the filter analogy, one can also define a cut-off frequency for the MEMS response to electrical stimulus. Again, the cut-off frequency is closely related to the MEMS process parameters, mass (m), and spring constant (k). If these parameters change, the cut-off frequency/resonant frequency of the system also changes. Eq. 2.5 shows the relation between the frequency and the process parameters.

$$\omega_0 = \sqrt{k/m} \qquad \text{Eq. 2.5}$$

3. Phase Shift

Simmilar to amplitude response, the phase shift between the input signal and the output response changes with different frequencies. The phase shift can be measured at the cut-off frequency. In later sections, it will be shown that the phase shift value at the cut-off frequency also changes when some changes in physical parameters occur.

4. DC offset

Every device starts off with a process induced DC offset in the differential capacitance when there is no physical or electrical signal being applied. As noted earlier, any applied signal will generate an additional offset. While DC offset cannot be directly measured and related to the offset in the differential gap, it can used in conjunction with other parameters to form the statistical model.

All the aforementioned electrical parameters were calculated from the simulations. Furthermore, some of them were measured during the hardware testing of the commercially available accelerometers. These parameters were then used to define an algorithm for creating a mathematical prediction model.

2.3 Summary of the chapter

1. An accelerometer model was designed in Simulink for physical and electrical stimulus testing.
2. Electrical simulation stimulus-based parameter extraction was discussed.

Chapter 3 CALIBRATION MODEL FORMULATION BASED ON SIMULATIONS

In this chapter, two different approaches for creating a prediction model will be discussed. The simulations will be done using the Simulink models explained in the previous chapters. The task will be to vary specific parameters of the accelerometer model and generate a sample set for further analysis.

3.1 Electrically inducing dc offset

As noted in the previous Chapter, the response of the MEMS device depends on the DC offset and magnitude of the applied electrical signal. The first approach is to take advantage of this property to generate multiple sensitivity measurements from a signal device and form a multi-variate correlation model that links the physical sensitivity to electrical response.

Monte-Carlo sampling was used to mimic process variations in mass (m) and the gap (d_0) between the plates and generate 100 device instances. In accordance with prior work [15] a 10% process variation model was used to generate the sample set. Then the sensitivities of these 100 different samples were calculated in terms of $\Delta C/V_{input}$.

For each of the generated samples, an offset of 50nm (i.e. an Δ=50nm) is introduced in the gaps between the two fixed plates. Based on the earlier observation, this would cause a shift in the sensitivity of each device. This effect can be observed in Fig. 3.1. Each device still displays a different sensitivity, but the sensitivities are shifted due to the change in the offset.

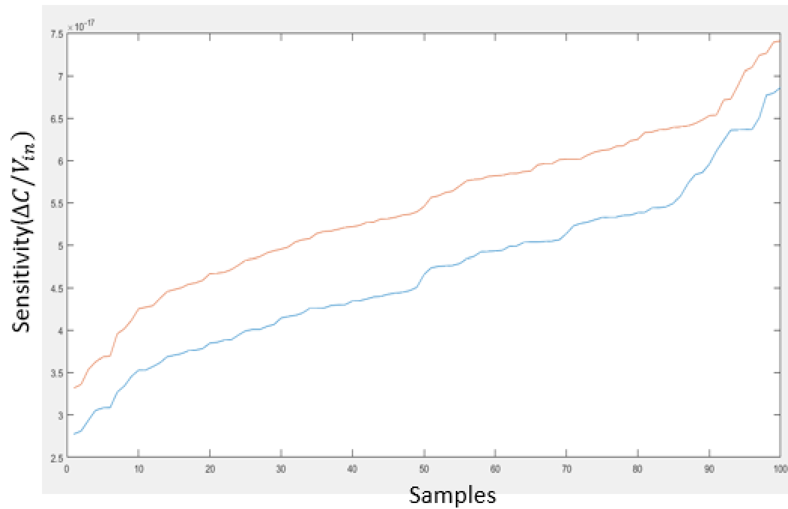

Figure 3.1 Sensitivity vs samples (Without and with an offset of 50nm)

Clearly, one cannot introduce a physical offset into the gap of the MEMS devices externally after it has been manufactured. But this offset can also be electrically induced by applying a constant electrostatic force (e.g. via a DC offset in the input signal or by changing the magnitude of the input). The first modeling approach takes advantage of this property. Electrical and physical parameters are measured for each of the device samples using different electrical DC offsets. The AC signal amplitude was kept constant, but the DC voltage was incrementally increased in steps of 0.1V. A flow chart describing the algorithm is shown in figure 3.2.

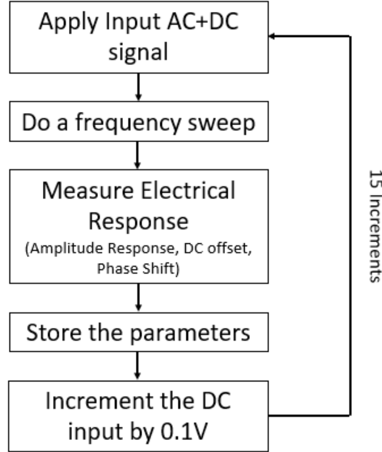

Figure 3.2 Algorithm for parameter extraction of incremental values of DC offsets

A trend was observed in the output electrical response when different offsets were applied. Figure 3.3 shows the relationship between the AC amplitude response of models with different DC values. This figure shows a clear correlation between the sensitivity and the electrical response. Moreover, now that there are multiple sensitivity measurements that can be conducted, a multi-variate model can be constructed. A first order model correlating the electrical response parameters to physical sensitivity is generated. For this model, the following electrical response parameters are used: amplitude response at low frequency (A_{low}), amplitude response at high frequency (A_{high}), phase shift(ϕ), amplitude roll off (A_{high}/A_{low}) and DC offset (V_{off}) [15]. This linear statistical model is given in Eq. 3.1.

$$S = c_1 + c_2 A_{low} + c_3 \left(\frac{A_{high}}{A_{low}}\right) + C_4 \phi + C_5 V_{off} \qquad \text{Eq. 3.1}$$

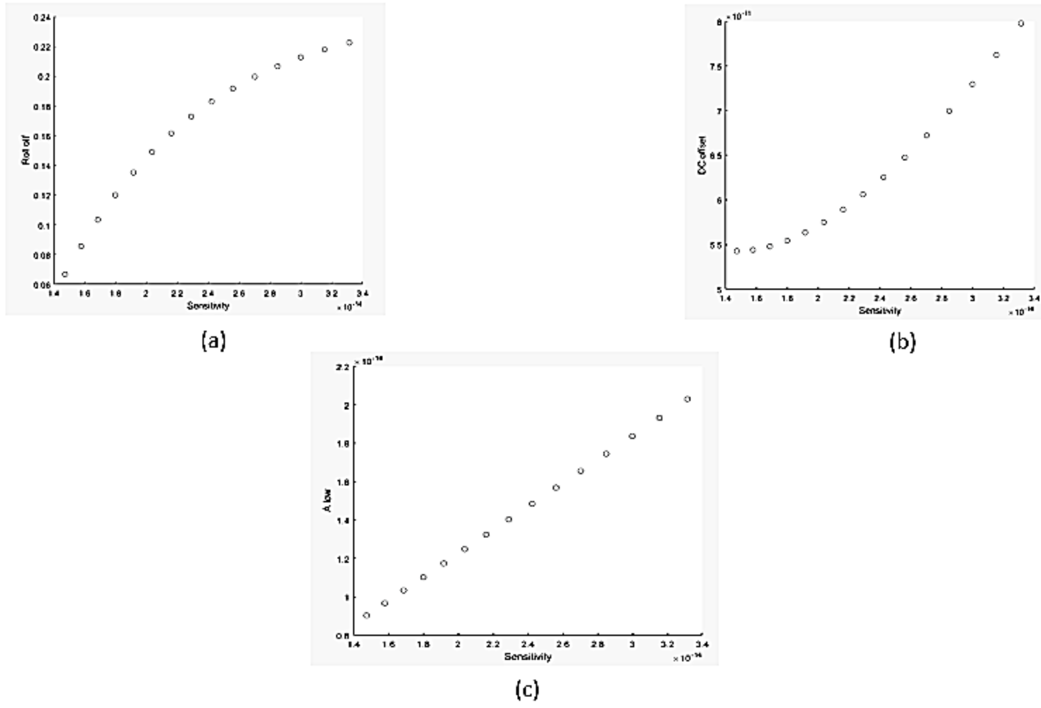

Figure 3.3 Sensitivity(F/g) Vs Electrical response(Roll off, DC offset(F), Alow(F))

The first order model of Eq. 3.1 provides an accuracy with an RMS error of 1%, which is the target for NIST traceability [18]. However, noting that there is accuracy degradation between simulations and hardware applications, it is desirable to increase the accuracy of the model. It is observed that the relations between the frequency roll-off and sensitivity and between the DC offset and sensitivity are non-linear. Thus, a second-order model is also developed for more accurate modeling. With this second order modeling, the RMS error in sensitivity prediction is reduced to 0.2%.

$$S = c_1 + c_2A_{low}^2 + c_3\left(\frac{A_{high}}{A_{low}}\right)^2 + c_4V_{off}^2 + c_5A_{low} * \left(\frac{A_{high}}{A_{low}}\right) + c_6A_{low} * V_{off} + C_7V_{off} * \left(\frac{A_{high}}{A_{low}}\right) \qquad \text{Eq. 3.2}$$

This prediction model was also used to predict the sensitivity of a sensor whose spring constant k has changed by 0.5%; the prediction error was 0.9%.

The benefit of this approach is that a prediction model can be generated independently for each sensor. The method is very simple to apply in the field with only electrical signaling and thus is suitable for BIST applications. Due to various wear out mechanisms, gap offset or spring constant of the MEMS device may change in the field and the model can be used to predict the new sensitivity to keep it within the NIST traceability standard [18].

However, to generate the multiple sensitivity measurements, it is necessary to increase the DC offset. Due to limited range of voltage that can be applied to the sensor, the range with which the DC offset can be introduced may also be limited. This in turn limits the range of sensitivity values that are obtained from the device. The differences in sensitivity are too small, the accuracy of the model will be reduced. Hence, depending on the application and the hardware parameters of the MEMS device as well as the analog and digital circuits connected to it, the approach may not be practical for all commercially available devices.

3.2 Sensitivity Degradation Model

As discussed in the previous approach, the model was defined on the electrically induced DC offset in the gaps of the fixed plates and the proof mass. There was only one type of variation that was taken into consideration. As it has been discussed in [12, 16] that with aging, accelerometer physical parameters can degrade and eventually lead to failure. The two of the parameters that can be affected are spring constant(k), which is dependent

on the material properties of the proof mass, and the gap offset (Δ), which could happen when the proof mass plate bends towards the plates and stays there.

In this approach for formulating a prediction model, the goal is to predict the degradation in sensitivity rather than the sensitivity itself from electrical measurements. The baseline sensitivity for each device is measured post-production. Hence, if the degradation in sensitivity is predicted, one can also predict the sensitivity at all times. To generate the training set, the same model was simulated but with incremental changes in k and Δ. 190 device samples were generated with the combinations of different delta values of k and Δ. For these models, the sensitivity of the device is measured using the physical stimulus simulation. The same device then is simulated with electrical stimulus. Changes in electrical parameters from the default values were measured for each sensor instances. The electrical parameters evaluated in this approach were, Cut-off Frequency (ω_0), Amplitude Response (C_0) and Phase shift (ϕ). The simulation algorithm is shown in Fig. 3.4.

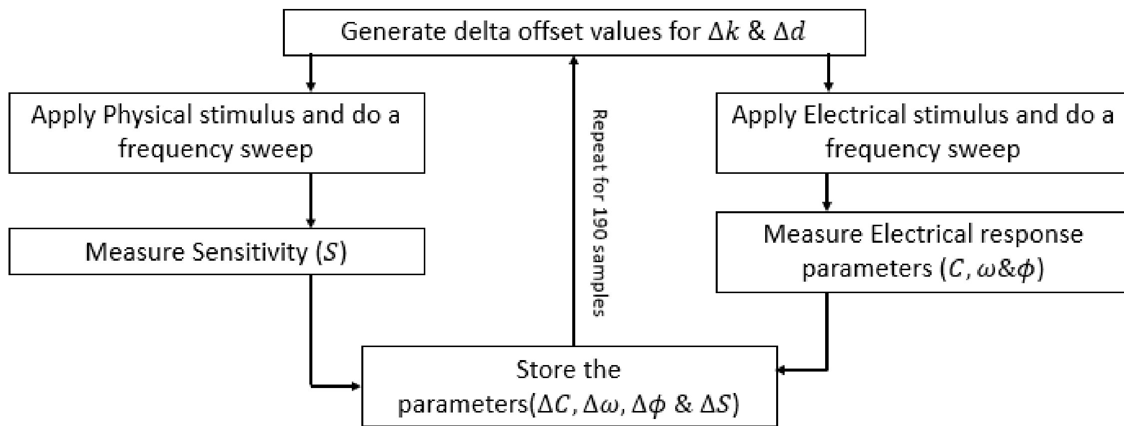

Figure 3.4 Delta change parameter extraction algorithm

After the simulations were run for all the 190 samples, the incremental changes in electrical parameters were plotted against the delta change in sensitivity from the default values. An observation was made that there is a trend in change in electrical responses when the spring constant (*k*) and gap offset was varied. Figures 3.5 show these relations.

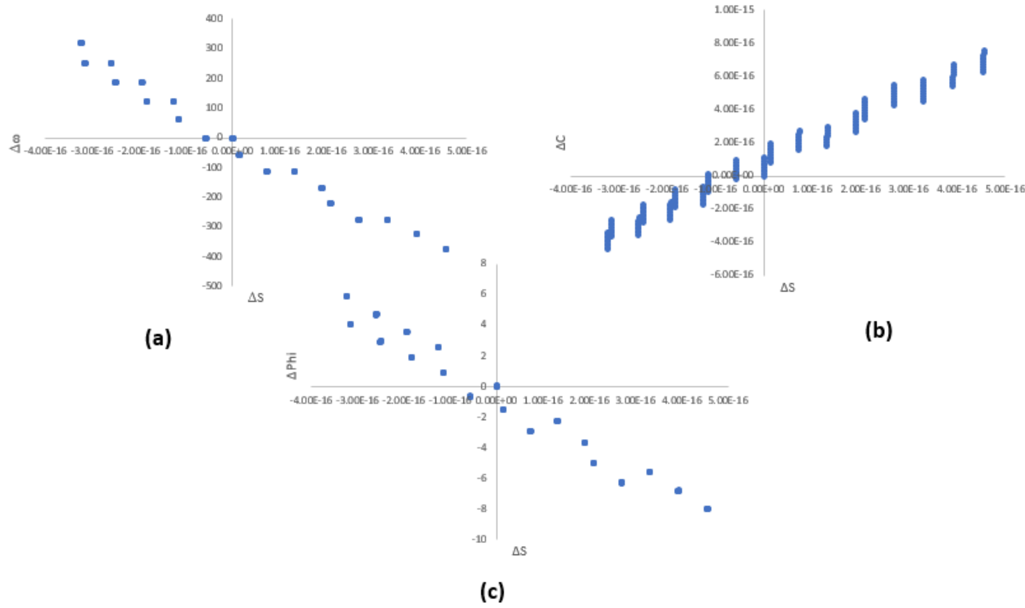

Figure 3.5 Delta change in electrical parameters(ω, C & ϕ) vs delta change in sensitivity

Linear regression was done on the data set to create a prediction model. The statistical model is presented in Eq. 3.3, where x_1, x_2, x_3 & x_4 are the fitting parameters for the model. After generating these fitting parameters, 100 randomly generated models were tested to check the accuracy of the prediction. The root means square error for this linear model was calculated to be around 1%.

$$\Delta S = x_1 + x_2 \Delta C + x_3 \Delta \omega + x_4 \Delta \phi \qquad \text{Eq. 3.3}$$

The idea behind this approach is to train a model for a specific set of sensors based on the degradation assumption. With the help of this model, a BIST circuit can be made to make infield prediction of the change in the sensitivity of a sensor.

3.3 Summary of the chapter

1. Electrical parameter response extraction was done for electrically induced DC offset models.
2. Statistical model formulation based on the incremental changes in sensor parameters.

Chapter 4 ACCELEROMETER HARDWARE TESTING

A commercially available MEMS accelerometer was used to evaluated the first approach of inducing a DC voltage offset and observing the change in the sensitivity. For the experimental set-up, a dual-axis accelerometer evaluation board (ADXL203EB) from Analog Devices was used. This sensor has a measurement range of $\pm 1.7g$, and the operating voltage range is 3V-6V. The factory provided a sensitivity of this sensor is 1V/g. There is a self-test pin input, which was used to apply an electrical stimulus to the sensor.

4.1 Only DC offset experiment

First, only a DC offset is applied as the electrical signal to determine if there is any variation in the sensitivity. A testing setup was 3D printed to orient the sensor in a position to get $\pm 1g$ acceleration. Figure 4.1 shows the test setup.

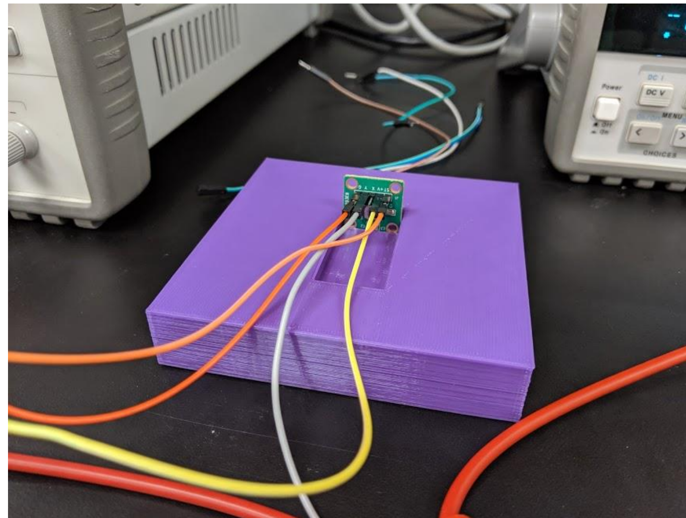

Figure 4.1 Test setup

Different DC voltages were applied to the self-test pin when operating under different supply voltages (V_{supply}). As the sensor can work in a 3V-6V operating range, all

the range was tested so that more data points can be generated. The DC voltage applied at the self-test pin was incremented in 1V steps starting from 0V and to $V_{supply} - 1V$. The sensitivity was measured physically by orienting the test setup differently to apply 0g,+1g, and -1g.

$$S_{physical} = (V_{(1g)} - V_{(-1g)})/2g \quad \text{Eq. 4.1}$$

The sensitivity for different DC offsets and supply voltages are shown in Table 4.1. It was concluded that the sensitivity change was not significant enough to be modeled.

Table 4.1 DC offset Sensitivity comparison

Operating Voltage(V)	Self-test Pin(V)	Sensitivity(V/g)
3	0	0.5598
3	1	0.5598
3	2	0.561
5	0	0.9985
5	1	0.9995
5	2	0.9981
5	3	1.00615
5	4	1.0062
6	0	1.25225
6	1	1.25195
6	2	1.25195
6	3	1.25225
6	4	1.25225
6	5	1.25195

4.2 AC and DC electrical stimulus

In the second run of testing, an AC signal was also applied along with a DC signal. This was done so that electrical parameters could be. First, testing was done for different supply voltages and increasing the steps of 0.5V starting from 3V. The AC response (V_{ac}),

DC response (V_{dc}), and sensitivities were calculated at a low frequency of 10Hz and a high frequency of 1kHz. The applied AC voltages and offset voltages were different for different operating voltages. This change was needed due to the varying ranges of input values at different supply voltage levels. For example, $V_{pp} = 1.5V \; and \; V_{off} = 0.75V$ were enough to induce an AC response for the supply voltage of 3V but was not enough for the supply voltage of 5V operating voltage. Table 4.2 shows the results of these measurements.

Table 4.2 AC and DC stimulus for different operating voltages

Operating Voltage(V)	Self-test pin(V)	V_{ac}(10Hz)	V_{ac}(1kHz)	Sensitivity(V/g)
3	$V_{pp} = 1.5 \; V_{dc} = 0.75$	65mV	4mV	0.5655
3.5	$V_{pp} = 1.5 \; V_{dc} = 0.75$	104mV	6.4mV	0.669
4	$V_{pp} = 2 \; V_{dc} = 1$	157mV	9.2mV	0.7795
4.5	$V_{pp} = 2 \; V_{dc} = 1$	227mV	13mV	0.89
5	$V_{pp} = 3 \; V_{dc} = 1.5$	315mV	17.6mV	1.00875
5.5	$V_{pp} = 3 \; V_{dc} = 1.5$	429mV	21.9mV	1.13
6	$V_{pp} = 3 \; V_{dc} = 1.5$	548mV	26mV	1.2605

Although a trend can be observed here, it was not confirmed if this trend in change in sensitivity was due to a change in operating voltage or due to the offset DC voltage signal. To test it out, another experiment was done. This time with a fixed operating voltage and fixed AC signal but changing DC offsets.

4.3 Fixed AC and different DC offsets

A DC offset was applied in incremental steps of 0.1V starting from 1V, with a fixed AC signal $V_{pp} = 1V$. For every DC offset, a frequency sweep was done from 1Hz to 1kHz,

to determine the electrical response of the system. Figure 4.2 shows the frequency response for different offset voltages.

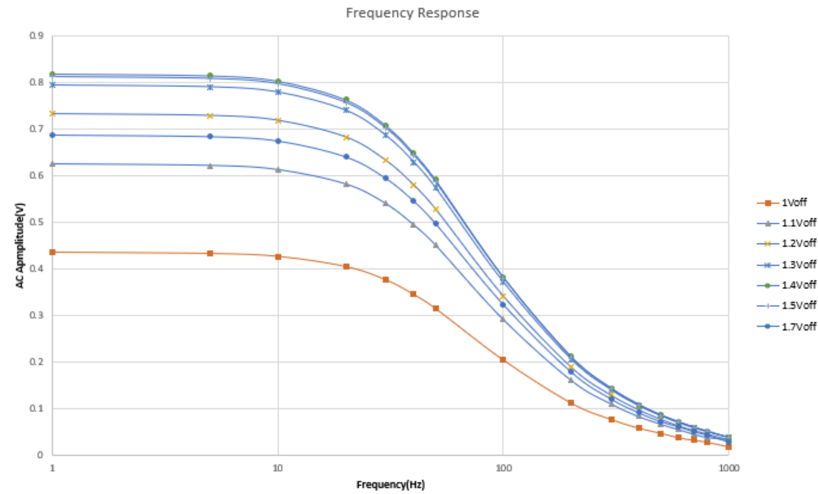

Figure 4.2 Frequency response for different DC offsets

It can be seen that the change in the frequency response shows a similar trend to that of the simulations. To determine if there was any trend in this change that can be modeled, amplitude responses at 50Hz frequency were analyzed. Figure 4.3 shows output signals for different DC offsets.

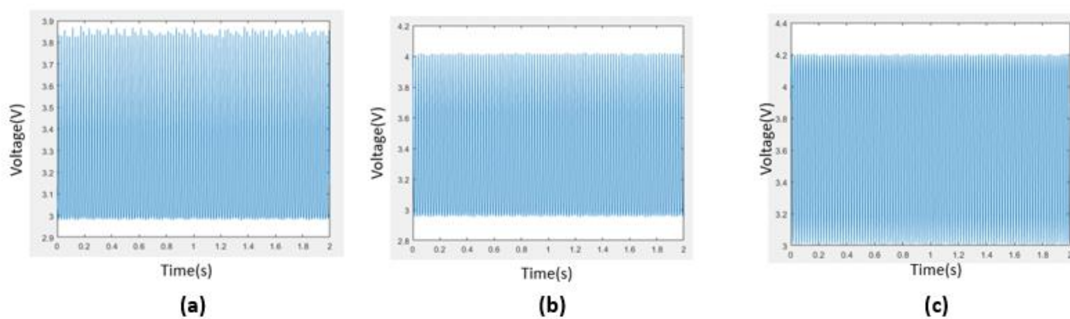

Figure 4.3 (a) 0Voff, (b) 1Voff & (c)1.5Voff

The change in sensitivity vs the AC response and output DC offset was plotted. A linear model was fitted on the data set to predict the sensitivity. The prediction error was calculated to be 0.2% of the actual measured sensitivity. The maximum change in sensitivity is 0.5%. In this experiment, the error and sensitivity degradation are close due to the limited dynamic range of the commercial device. This limitation has resulted in a very small range of change in sensitivity, thus increasing the relative error. However, these hardware experiments track the simulation results and show that different physical sensitivity can be induced for a given device using electrostatic force to enable multi-variate modeling.

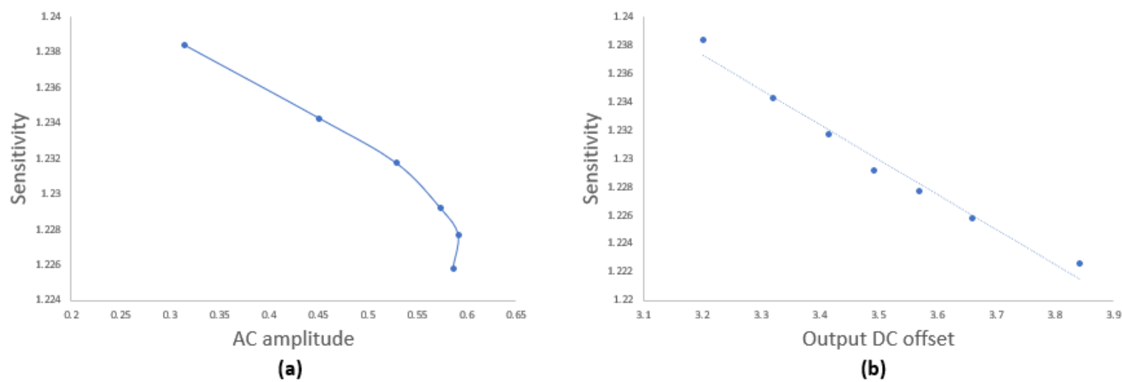

Figure 4.4 AC response and DC offset vs Sensitivity (Sensor 1)

The same prediction model was used on the electrical response of a second sensor, and a prediction was made. For the second sensor as well, a frequency sweep was done, and electrical responses were recorded. The physical sensitivity was also measured. The error in the prediction of sensitivity was 0.65%. This result shows that each device presents with its own sensitivity degradation model parameters. Hence, the prediction using the response from each device is more accurate than parameters used across devices.

4.4 Summary of the chapter

1. In this chapter, commercially available sensors were tested for electrical stimulus testing.
2. Different approaches to physical stimulus were tested.
3. Only DC offset was applied, and a change in sensitivity was observed.
4. A small AC signal was applied over different DC offset, and output parameters were analyzed.

Chapter 5 CONCLUSION AND FUTURE WORK

Electrical stimulus calibration can bring down the time, hassle, and cost of getting a sensor system back to the test facility for recalibration. As the sensors age, the sensitivity of the sensor degrades. This change in sensitivity can be modeled based on responses generated by the electrical stimulus. A statistical model can be developed by training it using the electrical responses from a sensor. Simulink simulations were done to extract the electrical parameters such as, amplitude response, phase shift, cut off frequency, and DC offset. These responses were recorded for different models generated based on changes in physical parameters such as, spring constant, gap offset in the plates. A prediction model was then generated based on these responses. Root mean square error of about 1% was recorded when the model was trained with 190 samples and tested for 100 samples.

Hardware testing was done on commercially available accelerometers to see if there was any change in electrical responses when different DC offsets were applied. A trend in change was observed during hardware testing.

For future work, the incremental change model, which is discussed in this work, will be tested out on hardware sensors. To introduce change in spring constant, the hardware will be treated under a high heat environment. The sensors will be placed in a controlled temperature, and then the electrical testing will be done. More sensors will be evaluated so that enough data can be gathered to make a prediction model, which then can be used for in-field calibration of accelerometers. The plan is to extend this same study to capacitive pressure sensors, for which some brief study has been done. These pressure sensors can

also respond to electrical stimulus, and a model can be formulated for their in-field calibration.

REFERENCES

[1] Senturia, S. D. (2007). *Microsystem design.* Springer Science & Business Media.

[2] Rasras, M., Elfadel, I. A., & Ngo, H. D. (2019). Editorial for the special issue on MEMS accelerometers. *Editorial for the special issue on MEMS accelerometers*. Multidisciplinary Digital Publishing Institute.

[3] Mohammed, Z., Elfadel, I. A., & Rasras, M. (2018). Monolithic multi degree of freedom (MDoF) capacitive MEMS accelerometers. *Micromachines, 9*, 602.

[4] Xiong, X., Wu, Y.-L., & Jone, W.-B. (2005). A dual-mode built-in self-test technique for capacitive MEMS devices. *IEEE Transactions on Instrumentation and Measurement, 54*, 1739–1750.

[5] Natarajan, V., Bhattacharya, S., & Chatterjee, A. (2006). Alternate electrical tests for extracting mechanical parameters of MEMS accelerometer sensors. *24th IEEE VLSI Test Symposium*, (pp. 6–pp).

[6] Allen, H. V., Terry, S. C., & De Bruin, D. W. (1989). Accelerometer systems with self-testable features. *Sensors and Actuators, 20*, 153–161.

[7] Rocha, L. A., Dias, R. A., Cretu, E., Mol, L., & Wolffenbuttel, R. F. (2011). Auto-calibration of capacitive MEMS accelerometers based on pull-in voltage. *Microsystem technologies, 17*, 429–436.

[8] Mir, S., Rufer, L., & Dhayni, A. (2006). Built-in-self-test techniques for MEMS. *Microelectronics journal, 37*, 1591–1597.

[9] Dumas, N., Azaïs, F., Mailly, F., & Nouet, P. (2008). Evaluation of a fully electrical test and calibration method for MEMS capacitive accelerometers. *2008 IEEE 14th International Mixed-Signals, Sensors, and Systems Test Workshop*, (pp. 1–6).

[10] Dumas, N., Azaïs, F., Mailly, F., & Nouet, P. (2010). Study of an electrical setup for capacitive MEMS accelerometers test and calibration. *Journal of Electronic Testing, 26*, 111–125.

[11] Ozel, M. K. (2017). *An Electrical-Stimulus-Only BIST IC For Capacitive MEMS Accelerometer Sensitivity Characterization.* Ph.D. dissertation, ARIZONA STATE UNIVERSITY.

[12] Gómez Pau, Á., Sanahuja Moliner, R., Balado Suárez, L. M., & Figueras Pàmies, J. (2012). Built-In test of MEMS capacitive accelerometers for field failures and aging degradation. *Proceedings of XXVIIth Conference on Design of Circuits and Integrated Systems*, (pp. 223–228).

[13] Xiong, X., Wu, Y.-L., & Jone, W.-B. (2008). Material fatigue and reliability of MEMS accelerometers. *2008 IEEE International Symposium on Defect and Fault Tolerance of VLSI Systems*, (pp. 314–322).

[14] Kundur, V. (2013). *An Electrical Stimulus based Built In Self Test (BIST) circuit for Capacitive MEMS accelerometer.* Master's thesis, Arizona State University.

[15] Ozel, M. K., Cheperak, M., Dar, T., Kiaei, S., Bakkaloglu, B., & Ozev, S. (2016). An electrical-stimulus-only BIST IC for capacitive MEMS accelerometer sensitivity characterization. *IEEE Sensors Journal, 17*, 695–708.

[16] Tewksbury, S. K. "Challenges facing practical DFT for MEMS." In Proceedings 2001 IEEE International Symposium on Defect and Fault Tolerance in VLSI Systems, pp. 11-17. IEEE, 2001.

[17] Douglass, Michael R. "MEMS reliability: coming of age." In Reliability, Packaging, Testing, and Characterization of MEMS/MOEMS VII, vol. 6884, p. 688402. International Society for Optics and Photonics, 2008.

[18] J.L. Marshall (1998), NIST Calibration Services User Guide.